https://doi.org/10.18322/PVB.2019.28.03.14-35 UDC 614.83;536.46

Effect of distance between ignition location and window on indoor gas explosion development

© Iurii Kh. Polandov^{1,2}, Sergey A. Dobrikov^{1,2}

- ¹ Orel State University named after I. S. Turgenev (Komsomolskaya St., 95, Orel, 302026, Russian Federation)
- MERA (Delovaya St., 13, Nizhniy Novgorod, 603163, Russian Federation)

ABSTRACT

Introduction. It has been previously known that for gas explosions in an unconfined chamber the following rule applies: the larger the distance between gas ignition location and relief opening (window), the higher the explosion pressure. This statement is based on results obtained by a number of researchers, including ourselves. However, as demonstrated by recent physical experiments, it is valid only for window sizes comparable to those recommended by guidelines to ensure certain safety conditions. For smaller window sizes, this relationship is leveled out or even changes its sign.

Research objective is to determine the cause of inversed relationship between distance from the window to ignition location and explosion pressure. Tackling this objective is of scientific and practical importance.

Research methods and tools. Two mathematical model variants for gas explosion development in an unconfined chamber were employed to study the revealed phenomenon, i. e. simplified model and numerical model. The first one, i. e. simplified model, is based on chamber representation as lumped volume, and using the Clapeyron equation in differential form. It was obtained that besides known factors, such as window size, properties of outflowing gases, etc., explosion development is influenced by the area of flame front and the time when it approaches the window. Unfortunately, this model does not take into account the dynamics of last factors development altogether. This task can be handled by the other model, numerical, implemented in Vulkan-M software. It is based on solving the gas dynamics equation system using large-particle method in Eulerian representation with added flame propagation conditions. Besides, Vulkan-M can visualize the physical process evolution, as well as record how its parameters and indicators develop.

Research results. It was found that if the window size is comparable to regulatory values, such a strong influence of window position on pressure is due not only to the difference of outflowing gas properties (initial mixture and combustion products), but also due to the fact that in the initial period of explosion development the flame front area is much larger for a further removed window than in case of a small distance between the window and ignition location. For a smaller window, the pressure increase rate in the initial period is high and almost identical for both explosion scenarios. Therefore, combustion time becomes decisive for the maximum pressure value. If the window is located far from the ignition, combustion time is shorter than in case of a smaller distance. As a result, maximum pressure in the second case is higher than in the first case. This explains the revealed phenomenon.

Conclusion. The larger the window size, the stronger it affects the explosion pressure. This influence is determined not only by gas outflow, but it intensifies, sometimes significantly, due to the influence on flame front development. If the window size is decreased, its influence on flame front development is weakened and becomes negligible. In this case, the explosion pressure is affected by combustion time, besides window size.

Keywords: deflagrational explosion, unconfined volume; explosion pressure; window size; window position; physical experiment; numerical experiment; flame front.

Acknowledgment. The authors acknowledge the support of Moscow State National Research University of Civil Engineering, Institute of Integrated Safety in Construction, in providing the facilities for carrying out physical experiments.

For citation: Iurii Kh. Polandov, Sergey A. Dobrikov. Effect of distance between ignition location and window on indoor gas explosion development. *Pozharovzryvobezopasnost/Fire and Explosion Safety*, 2019, vol. 28, no. 3, pp. 14–35. DOI: 10.18322/PVB.2019.28.03.14-35.

Iurii Khristoforovich Polandov, e-mail: polandov@yandex.ru

Introduction

It is generally accepted, as well as proven by experiment, that for gas explosions* increasing the distance between gas mixture ignition location and relief opening, or pressure relief window (further referred to as window), results in pressure rise, including its maxi-

mum value p_{max}^{**} . This result is widely known, and

However, the most impressive results were obtained on the Serjant plant [5], equipped with a chamber having

confirmed by us during tests in the chamber of 0.125 m³ in volume and 10 m³ with cubic shape [1, 2], as well as by our colleagues in the USA in a chamber of 63 m³ in volume [3], and by our British colleagues [4].

^{*} We consider a gas deflagrational explosion without flame-generated turbulence and resonant combustion.

^{**} We assume the maximum pressure value for the explosion.

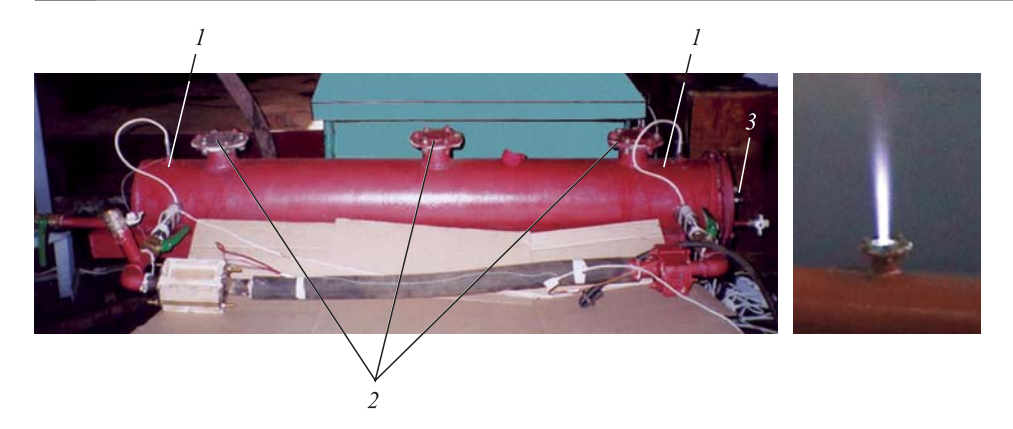


Fig. 1. General view of Serjant plant chamber and fragment of experimental explosion: I — pressure sensors; 2 — pressure relief windows; 3 — ignition device

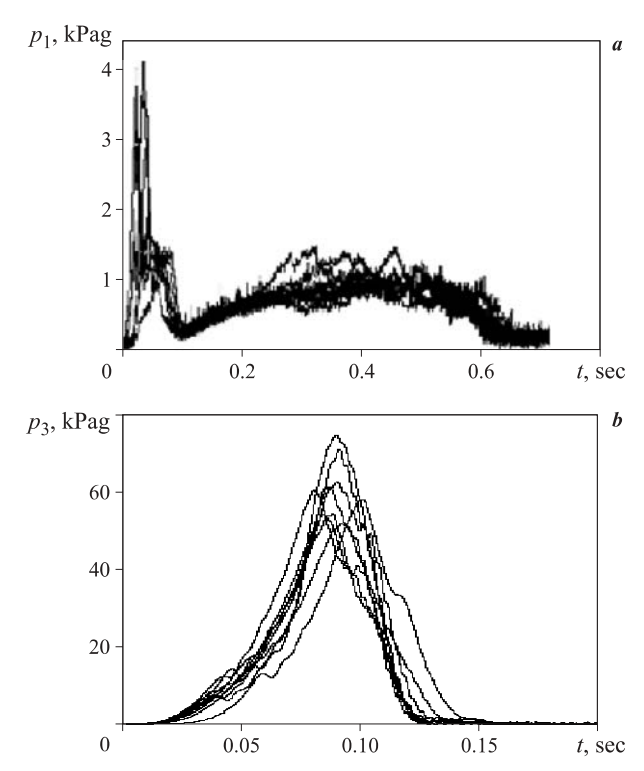


Fig. 2. Pressure course during explosions in a chamber with the window diameter of 60 mm in pos. 1 (a) and pos. 3 (b)

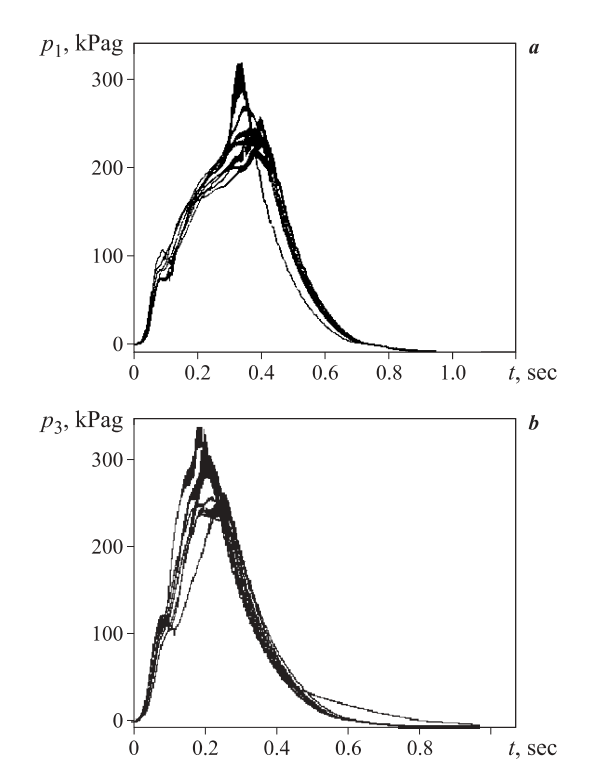


Fig. 3. Pressure course during explosions in a chamber with the window diameter of 20 mm in pos. 1 (a) and pos. 3 (b)

a length of l = 1.5 m and diameter of d = 200 mm (Fig. 1). This plant was used to study how window dimensions and position affect the explosion development. The chamber was filled by gas stoichiometric propane/air mixture. Research results are shown in Fig. 2 and 3 that provide combined data of 10 test runs for each of the variants. They demonstrate an acceptable level of results reproducibility which makes it possible to state that they are not random.

Further, it is assumed that in numerical experiments gas mixture is always ignited near the left flange*. Whereby, window location near this flange would be position 1, near the right flange it would be position 3, and in the chamber center — position 2. Correspondingly,

we shall designate the course of pressure that develops during explosion in a room with the window located in position 1 as $p_1(t)$, and with the window located in position 3 as $p_3(t)$.

From Fig. 2 one can see that $p_{\rm max}$ values for explosions in chambers with the window diameter of 60 mm installed in positions 1 and 3 will differ by more than 10 times, i. e. $p_{3\rm max} > 10p_{1\rm max}$.

However, other results obtained using the same plant, demonstrate that for the window diameter of 20 mm the dependence of p_{max} on window position is inverted (see. Fig. 3). Based upon the graphs in Fig. 2 and 3, one can see that, firstly, $p_3(t)$ pressure is significantly higher as compared to $p_1(t)$ (although it is evident, as the window size is reduced). Secondly, now $p_{3\text{max}} < p_{1\text{max}}$ (see Fig. 3), i. e. the sign of inequality is now in the opposite

^{*} In the physical experiment (see Fig. 1), ignition was initiated on the right-hand side.

direction. One should also note that pressure peaks have moved closer to each other: $p_{3\max}$ occurs earlier than $p_{1\max}$.

Hence, the objective has been set to identify why the influence of window location on gas explosion development is inverted if its dimensions are modified. Solving this objective is not only of scientific, but also of practical significance.

Working hypothesis

Obviously, in a confined space (no window) the window's influence on flame development is non-existent, while in a chamber with a window it is present. Hence, it is logical to formulate a premise that a larger window size produces a stronger influence on the explosion process. However, it is affected not only by the window size but also by other explosion development conditions. Primarily, this refers to the window position (including distance) relative to the gas mixture ignition location.

Still, it is impossible to explain the revealed phenomenon if only the window size and outflowing gas properties are known. Actually, even if one could interpret the deviation between $p_1(t)$ and $p_3(t)$ with explosions in a chamber with the window diameter of d=60 mm as caused by the difference between initial mixture and combustion products properties, it is not possible for explosion results in a chamber with the window diameter of d=20 mm, when $p_3(t)$ is greater than $p_1(t)$. It only remains to suppose that apart from window size and outflowing gas properties there are other factors that affect the explosion process. Their range can be determined by analyzing the mathematical models of explosion.

Simplified mathematical model

Due to the fact that the revealed dependence is primarily typical of cylindrically-shaped chambers with a high l/d ratio (which equals 7.5 for the Serjant plant), subsequent studies are conducted in this chamber.

Firstly, let us consider a widespread and in many ways simplified model of indoor explosion on the assumption that pressure is the same in all points of the room or, as certain authors refer, on the assumption of a quasi-static or quasi-stationary pressure in the room [5, 6]. It should be noted that these terms are ill-suited for this purpose, because they are already known in physics and mechanics and are used in a different context. At the same time, mechanics operates the notion of distributed and lumped parameters, such as mass. Similarly, in our case one could also refer to lumped volume, represent the chamber volume as a point and assign gas parameters to it. Besides the above-mentioned important assumption, we shall also assume that gas composition remains unchanged despite the chemical reaction that takes place during burning*, and that gas properties are ideal. Then, the equation of state will be valid for the gas mixture in the chamber

$$pV = MRT_{av}, (1)$$

where p is pressure, Pa;

V is the chamber volume, m^3 ;

M is the mass of gases involved in the process, kg; M = const;

R is gas constant, $J/(kg \cdot K)$;

 T_{av} is the mean temperature value of gases in the chamber, K.

Let us perform a differentiation of equation (1) on time. We shall also note that it is valid if the gas quantity remains unchanged (mass is the same), although, at first glance we are dealing with gases flowing out of the chamber, i. e. with variable mass. However, if we consider that the outflowing gas is essentially the volume's expansion and a part thereof, then the value of gas mass remains conditionally constant. It is worth mentioning that some authors believe that the explosion process and gas expansion in the chamber take place according to the adiabatic law [6, 7], whereas others agree that the explosion results in varying mass of gases present in the chamber [8]. In the first case, the authors' error stems from the fact that gas temperature increases not only adiabatically but also as a result of combustion, i. e. the explosion process is a polytropic one. The second case violates the rule of invariable mass of gases involved in the process. This is wrong because it precludes from using the equation of gas state.

Let us proceed to the differential form of equation (1):

$$\frac{\mathrm{d}p}{\mathrm{d}t} = -\frac{p}{V}\frac{\mathrm{d}V}{\mathrm{d}t} + \frac{MR}{V}\frac{\mathrm{d}T_{av}}{\mathrm{d}t}.$$
 (2)

The first term on the right-hand side of equation (2) uses the derivative value to express the intensity of volume expansion and is obtained via volume flow:

$$dV/dt = F_0 w, (3)$$

where F_0 is effective window area, m²;

w is outflowing velocity, m/sec.

Three cases can be differentiated for gases outflow depending on chamber pressure. Outflowing velocity will be determined for these cases using the following formulas:

1) when $p \le 0.2p_a$ (where p_a is atmospheric pressure, Pa), outflowing gas can be assumed as incompressible liquid:

$$w = \sqrt{2(p - p_a)/\rho_i},$$
 (3.1)

where $\rho_i = \rho_1$ is initial gas mixture density in the chamber, kg/m³;

 $\rho_i = \rho_2$ is combustion products density in the chamber, kg/m^3 ;

^{*} The error introduced into the gas constant value is 3 % max.

2) when $0.2p_a (where <math>p_{cr}$ is the critical outflow pressure, MPa; $p_{cr} \approx 0.19$ MPa), subcritical outflow occurs:

$$w = \sqrt{\frac{2k}{k+1}} \frac{p}{\rho_i} \left(1 - \frac{p_a}{p} \right)^{\frac{k-1}{k}}, \tag{3.2}$$

where k is the adiabatic value; $k = C_p/C_v$; k = 1.4 for the initial mixture, k = 1.25 for combustion products;

the value of 2k/(k+1) ratio varies insignificantly: from 1.11 to 1.16 during combustion products and initial gas mixture outflow, correspondingly;

3) when $p \ge p_{cr}$, the outflow becomes critical:

$$w = \sqrt{\frac{2k}{k+1} \frac{p}{\rho_i}} = \beta \sqrt{\frac{p}{\rho_i}}, \qquad (3.3)$$

where $\beta = \sqrt{2k/(k+1)}$ changes only slightly (between 0.64 and 0.68 during combustion products and initial gas mixture outflow, correspondingly).

Further. In the second term on the right-hand side of equation (2) the mean chamber temperature value T_{av} is defined as a weighted average due to the additivity of gas mixture properties:

$$\begin{split} T_{av} \; &= \frac{M_1 T_1 \; + M_2 T_2}{M} = \frac{\left(M - M_2\right) T_1 \; + M_2 T_2}{M} \; = \\ &= T_1 \; + \frac{M_2}{M} \left(T_2 \; - T_1\right), \end{split}$$

where M_1 , M_2 is the mass of initial gas mixture and combustion products, correspondingly, kg;

 T_1 , T_2 is the temperature of initial gas mixture and combustion products, correspondingly, K.

Therefore, as T_1 and T_2 are the energy characteristic of this mixture, and their values are known:

$$T_2 - T_1 = q/C$$

derivative value dT_{av}/dt will be determined as

$$\frac{\mathrm{d}T_{av}}{\mathrm{d}t} = \frac{T_2 - T_1}{M} \frac{\mathrm{d}M_2}{\mathrm{d}t} = \frac{q}{CM} \frac{\mathrm{d}M_2}{\mathrm{d}t} ,$$

where q is gas mixture calorific value, J/kg;

C is gas mixture specific heat capacity, $J/(kg \cdot K)$.

Let us take into consideration that $dM_2/dt = U_n F_f \rho_1$. Then

$$\frac{\mathrm{d}T_{av}}{\mathrm{d}t} = \frac{q}{CM} U_n F_f \rho_1, \tag{4}$$

where U_n is normal combustion rate, m/sec;

 F_f is flame front area, m².

By applying values from (3) and (4) to equation (2), we obtain:

$$\frac{\mathrm{d}p}{\mathrm{d}t} = -\frac{p}{V} w F_0 + \frac{MR}{V} \frac{q}{CM} U_n F_f \rho_1.$$

Let us rearrange this equation taking into account that

$$\rho_1 = \rho_{1a} (p/p_a)^{1/k},$$

then we obtain the final equation that connects the rate of pressure rise (or fall) to the critical process indicators:

$$\frac{\mathrm{d}p}{\mathrm{d}t} = -\frac{p}{V} w F_0 + \frac{R}{V} \frac{q}{C} \rho_{1a} \left(\frac{p}{p_a}\right)^{1/k} U_n F_f, \qquad (5)$$

where ρ_{1a} is initial mixture density under normal pressure, kg/m³; $\rho_{1a} = 1.22 \text{ kg/m}^3$.

Calculation of maximum explosion pressure

Physical experiments demonstrate that, generally speaking, there are several scenarios when explosion pressure arrives at its peak value $p_{\rm max}$ (sometimes locally). Firstly, this occurs when ${\rm d}p/{\rm d}t=0$, i. e. when summands in the right-hand side of equation (5) are equal; secondly, when the outflowing initial gas mixture is replaced by combustion products; thirdly, when the flame front area is abruptly changed (reduced).

Let us consider the first scenario, as it can be approached analytically, using equation (5). The other two variants when $p_{\rm max}$ maximum pressure occurs will be considered using specific examples in the analysis of numerical experiment results.

When the maximum pressure is calculated with the balanced right-hand side of equation (5), the expression for critical outflow is relatively simple ($p = p_{\text{max}}$ with the known value of k):

$$\frac{p_{\text{max}}}{V} \beta \sqrt{\frac{p_{\text{max}}}{\rho_i} p_{\text{max}}^{-1/k}} F_0 = \frac{R}{V} \frac{q}{C} \rho_{1a} p_a^{-1/k} U_n F_f, \quad (6)$$

whence

$$p_{\text{max}} = \left[\left(\frac{F_f}{F_0} \frac{Rq}{C\beta} \rho_{1a} U_n \right) p_a^{-1/k} \rho_i^{0.5} \right]^{\frac{k}{1.5k - 1}}.$$
 (7)

With k = 1.4

$$p_{\text{max}} \cong \left(\frac{F_f}{F_0} \frac{Rq}{C\beta} \rho_{1a} U_n\right)^{1.27} p_a^{-0.91} \rho_i^{0.635}.$$
 (8)

According to this relationship, decrease in outflowing gas mixture density from 1.22 to 0.17 kg/m³ (after combustion) can result in the maximum chamber pressure dropping by 3.5 times. However, this is true only when other conditions of explosion development are identical for the cases being compared. This is hardly possible as change in one parameter leads to changes in other parameters.

One can also raise another question: if, with other things equal, but with different outflowing gas temperatures, the chamber pressure is still the same, then what should the ratio of flame front dimensions be in both cases? From equation (8) it follows that $F_{f1}/F_{f2} = (\rho_2/\rho_1)^{0.5}$, hence in our case we obtain the ratio $F_{f2} = 2.65F_{f1}$.

As far as subcritical outflow scenarios are concerned, the relationship $w = w(\rho_i)$ assumes a more complex form in these variants, hence its solution is not given here. In principle, it is sufficient to analyze formulas (3.1)–(3.3) that express the outflowing velocity. All of them include the outflowing gas density in the form of factor $\rho_i^{-0.5}$, hence a relationship similar to (7) is to be expected. Obviously, one should treat formula (7) as an approximation, as many indicators it includes vary during the explosion process, albeit slightly. Unfortunately, conditions that allow to apply this formula, are rarely met.

On factors that affect flame front development

The influence of flame front area F_f on explosion development according to formula (5) is evident, hence researchers give sufficient attention to this matter. Speaking about the dynamics of this critical parameter, we shall note that flame-generated turbulence is not taken into account in line with the assumption made. Moreover, based on numerical experiment results it is not observed in the chamber of Serjant plant. The notion of how laminar flame develops is well known. Visible flame front is formed due to its movement with the speed determined by three processes: combustion itself, gas expansion during heating, and gas flow movement towards the window in order to be discharged.

Firstly, as early as in the 19th century, since the time of Russian scientist V. A. Mikhelson, it has been known

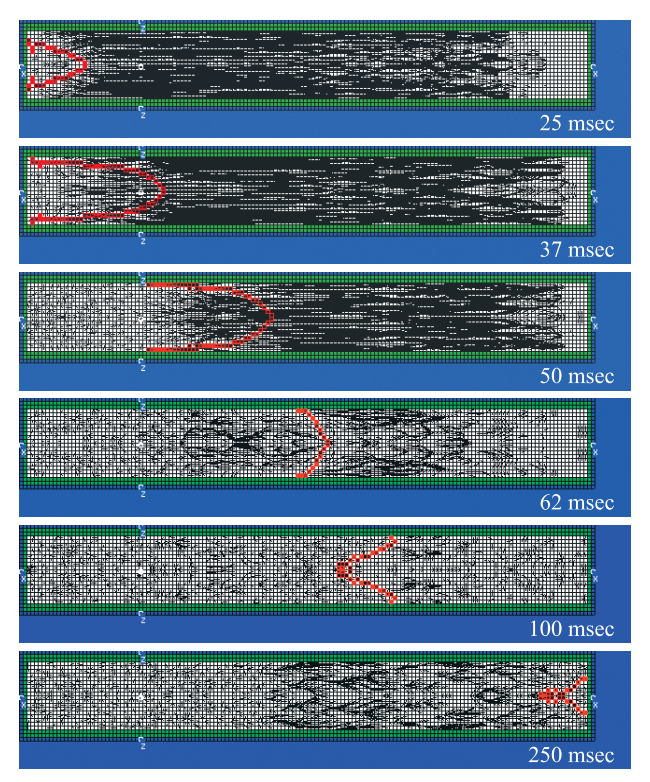


Fig. 4. Explosion in Serjant plant confined volume

that for laminar flame the vector of combustion velocity in gas is directed normally towards the front surface. Propagation rate is typically a few tens of centimeters per second. In our case, for propane/air mixture it is between 0.38 and 0.42 m/sec.

Secondly, gas expands in the combustion area, and contracts outside this area on both sides of it. This results in movement of gases away from the combustion area, including movement of flame front. Front velocity modulus is the higher, the larger the volume of gas layer located on the side that this vector is directed to. This process is clearly observed during numerical gas explosion modeling in the confined chamber of Serjant plant. It is especially typical of the initial time of explosion development (Fig. 4). One can see from the figure that along the chamber axis front velocity assumes a value larger than velocity towards the chamber wall, forming a well-known semi-elliptical shape of flame.

Thirdly, gas outflow also affects the flame shape. It is known that gas flow in a cylindrical volume under laminar conditions has a velocity profile resembling a semi-ellipsoid elongated in the discharge direction.

In a gas explosion, all of these velocity vectors are combined according to the superposition principle.

Gas explosion numerical modeling

A feature of describing gas explosions by means of numerical methods is that they provide a possibility to calculate gas parameters when distributed over volume. This provides for tracking not only pressure and temperature variations in all computation cells which the volume is divided into, but also flow velocity and flow paths. Besides, by modeling flame propagation conditions from cell to cell, it is possible to observe the development of flame front, a fundamental parameter that defines how an explosion evolves. For this purpose, we revert to numerical explosion modeling in the Serjant plant chamber. It was completed according to the input data, using the domestically produced Vulkan-M software [9, 10] developed on the basis of large-particle method [11].

Explosion modeling in Serjant plant confined volume

To analyze numerical modeling results, it is practicable to take into account the outcomes of gas explosion calculation performed on the Serjant plant with the confined chamber volume. This numerical experiment with flame front visualization acts as a homing experiment. It may also be assumed as a control experiment in terms of evaluating the performance of Vulkan-M software tool. The process inside a chamber filled with gas mixture of stoichiometric composition is being modeled. Mixture ignition occurs on the left of flange with reference to the chamber centerline. Trial results are

given in Fig. 4–6. The computational volume is divided into approximately 50,000 cells of cubic shape with the edge length of 1 cm. Flame front is represented by burning cells shown in red color. Fig. 4 illustrated a typical pattern of front development. At first, it rapidly expands into a semi-ellipsoidal shape. As a result, it acquires maximum area. Then, having grown to half the volume, it degrades into a plane. This is explained by the fact that in this case the chamber space on both sides of the flame front, where compression occurs, has the same dimensions. As a result, their elasticity is identical. In the second half of the volume the front acquires a shape that is for some reason referred to as "tulip", although it more likely resembles a funnel, whose drain channel is directed towards the combustion products side. Visible front traveling speed is much slower in this part: it needs 60 msec to travel the first part, while 200 msec are needed for the second part.

Pressure and flame front area calculation results are given in Fig. 5. The figure demonstrates that the front area reaches its maximum value in 50 msec. This is in line with "visual" data shown in Fig. 4. While the flame front is moving in the first part of the volume, the pressure increases at a very high rate. As it approaches the middle, it is falling fast. This is due to the fact that initial gas mixture volume is compressed the more inten-

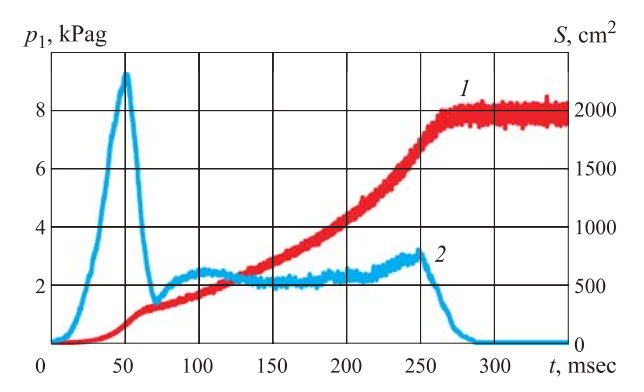


Fig. 5. Dynamics of pressure and flame front area development for a confined volume explosion

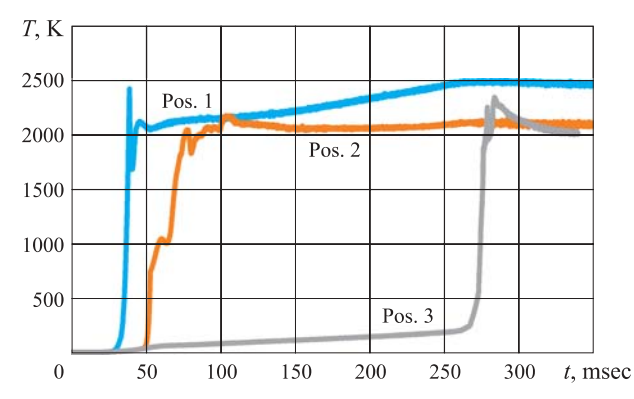


Fig. 6. Dynamics of gas temperature for a confined volume explosion: "sensors" at the left flange (pos. 1), in the chamber middle (pos. 2) and at the right flange (pos. 3)

sively, the larger its volume and the lower the chamber pressure, as dV/dp = -V/(kP). This is characteristic of the primary stage of flame front development. From Fig. 6 one can see that the flame front area at point 50 msec starts decreasing after touching the chamber walls, as the flame does not spread in the radial direction. At point 75 msec, the front crosses the chamber middle line. Data shown in Fig. 5 and 6 clarify the video frames on Fig. 4.

Explosion in Serjant plant with the window diameter of 60 mm

Fig. 7 and 8 demonstrate numerical experiment results of gas explosions in a chamber with Serjant-type geometry. Experiments were carried out with the window successively located in two points — near ignition location (position 1) and on the opposite side (position 3). Fig. 9 shows the behavior of pressure curve $p_1(t)$ with the window in position 1 and $p_3(t)$ with the window in position 3. Let us compare them with the results of physical experiments (see Fig. 2). Performance of a mathematical model is confirmed not only by the qualitative agreement on numerical and physical experiment results, but to a large extent by their quantitative concurrence. It is clear that not only is the process duration almost identical, but the behavior of curves in general is very closely matched. Thus, we can quite safely accept the data obtained in the numerical experiment on flame front development and use them for analysis (see Fig. 7 and 8).

Window position 1. As shown in Fig. 7, after touching the chamber wall, the flame front very quickly reaches the window. Combustion products are also discharged, hence initial mixture is finally combusted in the window and outside the chamber. Due to this fact and to almost identical velocities which the front travels with to the right side (by compressing the unburnt part of the mixture) and to the left side (due to the velocity of gases rushing towards the window), front position and size somewhat stabilize and remain practically unchanged up to t = 200 msec. At this time the front area remains as small as possible, i. e. close to the chamber cross-section area.

At the lapse of 200 msec the front detaches from the window and slowly moves to the right, growing in area, that achieves its maximum value at point t = 450 msec. The front area decreases when it touches the right end.

As shown in Fig. 9a, pressure $p_1(t)$ has two peak values. The first one is produced due to intense flame front expansion, typical for the initial stage of its propagation, that results in the growth of chamber pressure. Then, when the front simultaneously reaches the chamber walls and window, combustion products along with a part of the flame start discharging through the front. As a result, pressure drops abruptly. The second peak is also related to a variation in flame front

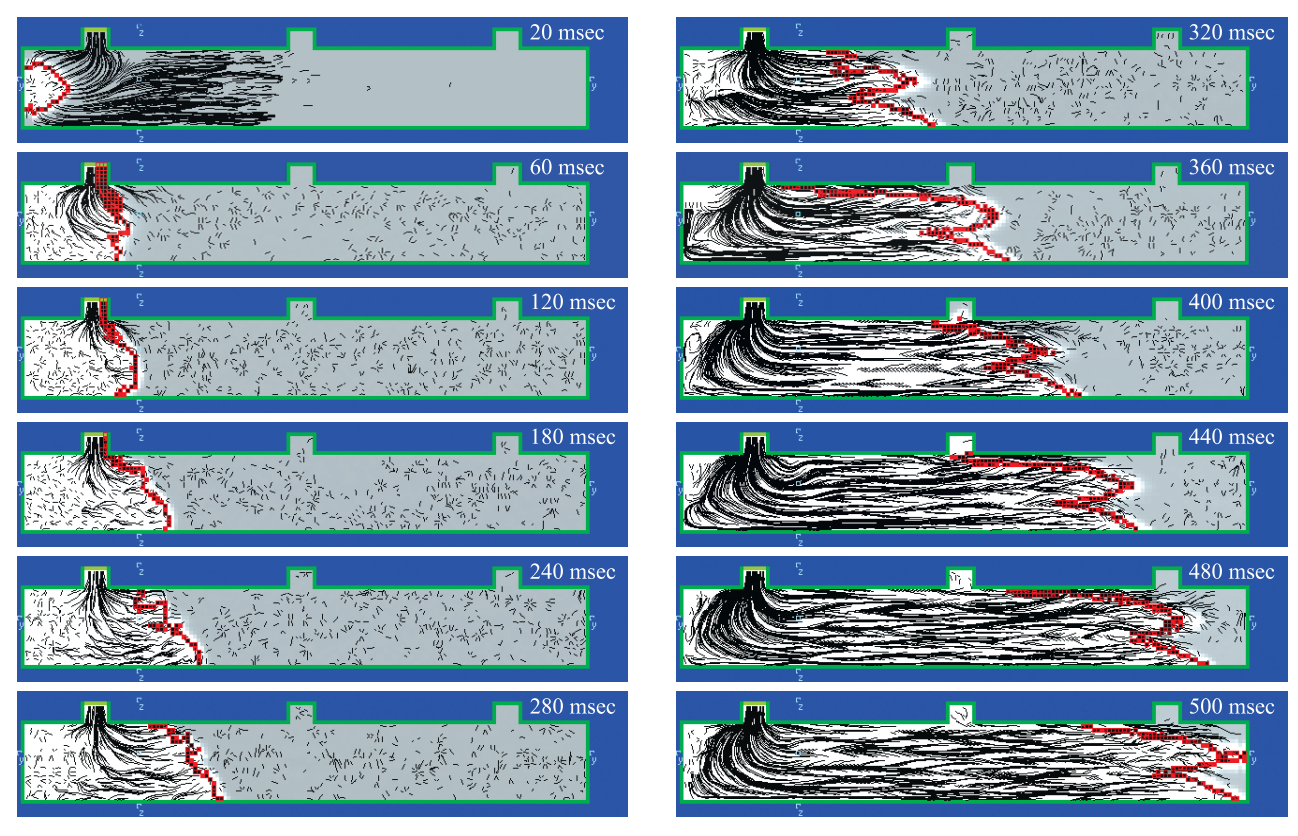


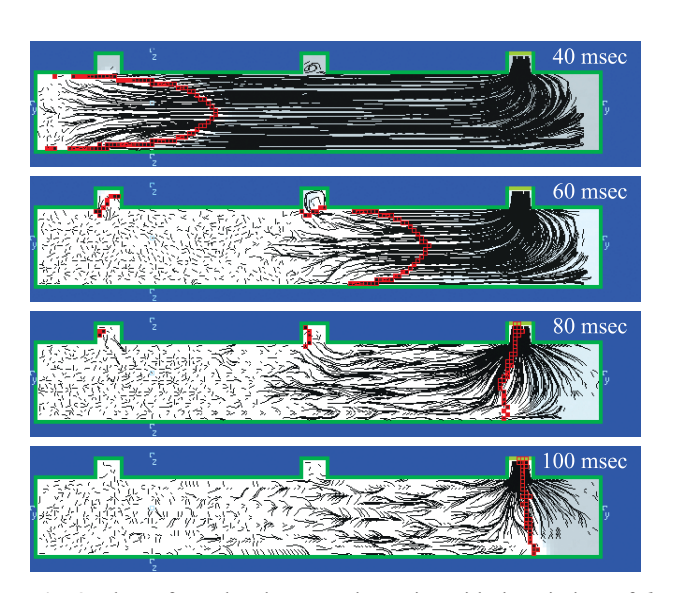
Fig. 7. Flame front development dynamics with the window of d = 60 mm in pos. 1

area. In this case, the area is growing within the time interval of 250 to 500 msec. Having reached its peak, it decreases (see Fig. 7 and Fig. 12 further).

Window position 3. In this case, the pattern of flame front development is completely different (see Fig. 8). Here, velocities of combustion, gas compression and gas mixture flow movement towards the window are combined. As a result, the flame front that initially has an ellipsoidal shape, is strongly elongated and drawn to the window which the initial mixture is flowing through. Despite the fact that it flows at a lower speed than com-

bustion products do, the front moves towards the window very rapidly, and it reaches the window in 80 msec. After that the front velocity slows down, and it takes the same 80 msec to cover the final 10 % of space. At this time, the pattern of flame front development represented in Fig. 7 for the initial period is repeated. This observation is further confirmed by the graph in Fig. 12.

In Fig. 9b, it is evident that pressure $p_3(t)$ increases up to point 70 msec; in this period of time the initial mixture is outflowing. After combustion products are discharged through the window, pressure drops and it is



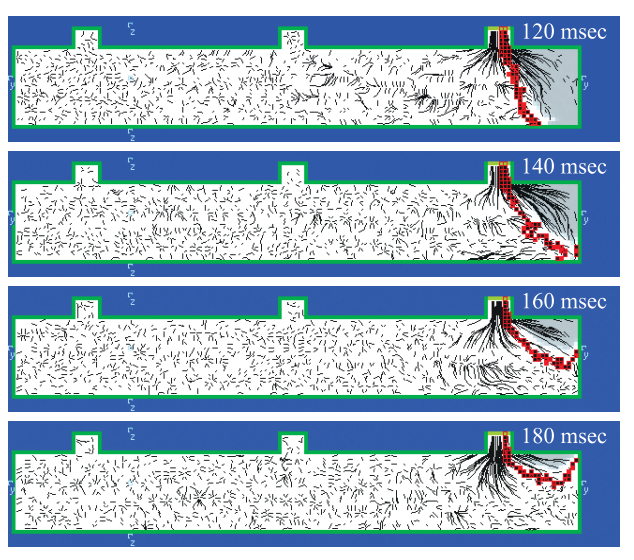


Fig. 8. Flame front development dynamics with the window of d = 60 mm in pos. 3

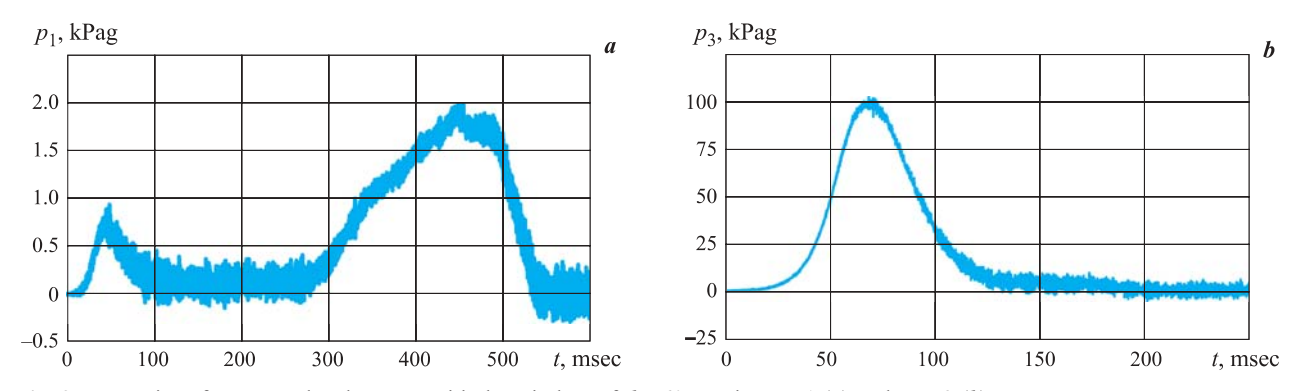


Fig. 9. Dynamics of pressure development with the window of d = 60 mm in pos. 1 (a) and pos. 3 (b)

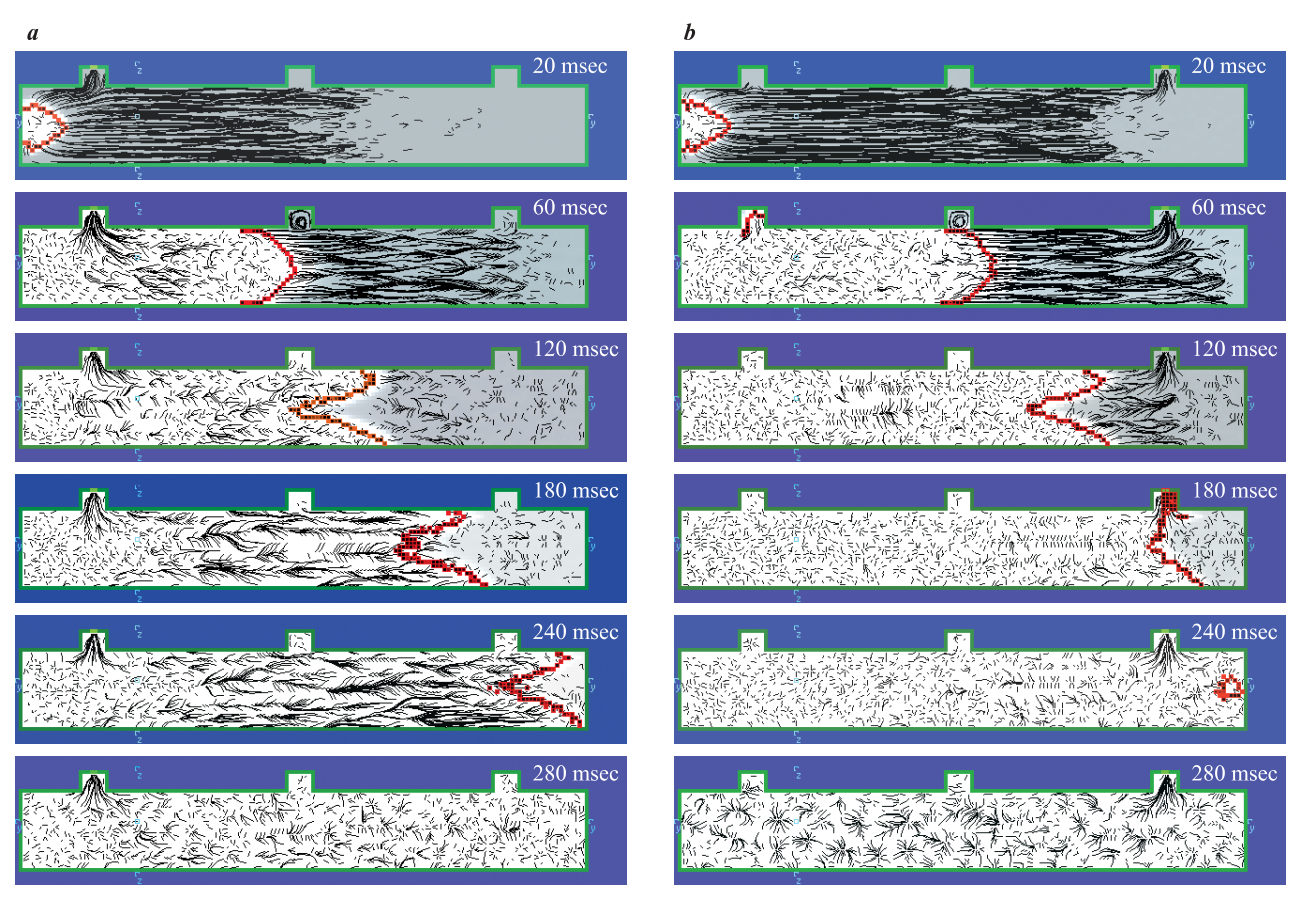


Fig. 10. Dynamics of flame front development for explosion in the chamber with the window of d = 20 mm near left end (a) and right end (b)

almost equal to zero within the time period of 120 to 180 msec. In this case, the duration of explosive process is much less than in the first case. The mathematical model demonstrates that in the scenario with the window positioned near the ignition location the initial mixture is combusted almost completely. However, when the window is positioned at the far flange, more than 90 % of initial mixture is discharged from the chamber.

Explosion in Serjant plant with the window diameter of 20 mm

Reducing window diameter to 20 mm results in a qualitative change in the way it affects the explosive

process (Fig. 11). With the smaller window size, the pattern of flame front development becomes closer to its behavior in a confined chamber. This is noticeable when comparing the frames in Fig. 10 and 4 to each other. This is also demonstrated by how close the process duration values are for window positions 1 and 3 (see Fig. 12).

Pressure in the chamber grows in the same manner with both window position options until the flame front touches the chamber walls. After that the graphs diverge, so that chamber pressure with the window position 1 will always be higher than with position 3, i. e. $p_3(t) > p_1(t)$, which is explained by the influence of outflowing gas properties. However, at $p_3(t)$ the flame front

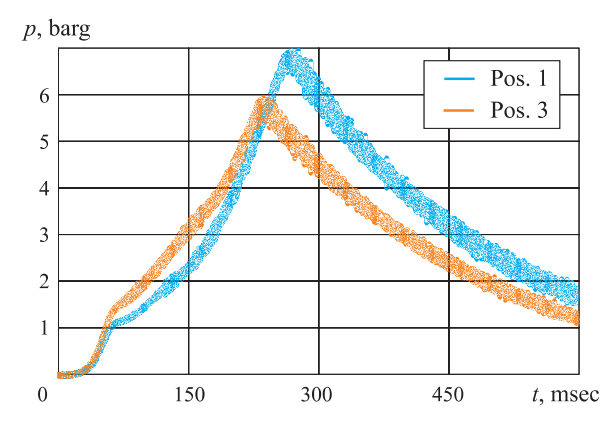


Fig. 11. Dynamics of pressure development with the window of 20 mm in pos. 1 and pos. 3

reaches the far end earlier than at $p_1(t)$, as the effect of velocities combination is manifested. By the point of 180 msec combustion stops and the chamber starts emptying.

At the same time, with the window in position 1, the flame front moves at a slower speed. Combustion continues even after it has completely stopped in the case with window position 3. Hence, pressure $p_1(t)$ continues to grow after $p_3(t)$ has already started falling. As a result of a longer combustion time, maximum value $p_{1\max}(t)$ is greater than $p_{3\max}(t)$. Having touched the right end, the flame front at $p_1(t)$ starts abruptly contracting. Combustion stops and the chamber starts emptying at almost the same rate as in scenario with $p_3(t)$. Pressure maximums are produced in the same manner in both cases: pressure in the chamber grows during combustion and falls after it has stopped, thus forming a pressure peak.

Dynamics of flame front areas development

The numerical model also provides for assessment of flame front area. The model assumes that flame front thickness is defined by the linear cell dimension, while its area $S(m^2)$ is calculated based on the cell edge area. Then

$$S = n S_1$$
,

where *n* is the number of burning cells;

 S_1 is the edge area of a computational cell, cm²; in our case $S_1 = 1$ cm².

Fig. 12 compares the dynamics of flame front areas development occurring in each of the four above-mentioned experiments. From Fig. 12, one can see that in all scenarios at the beginning of front development (up to the time point 5 msec) pressure rise occurs in the same manner. All graphs concur, but further they start to separate. The first one to decrease is the front area with the window diameter of 60 mm located in position 1. This is due to the fact that the flame front reaches the window and a part of the flame front starts

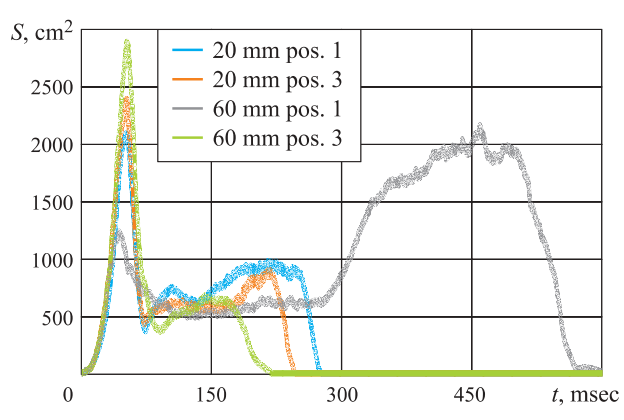


Fig. 12. Dynamics of flame front development with the window of 20 mm and 60 mm in pos. 1 and pos. 3

flowing out through the window along with combustion products. At the same time, flame with the window diameter of 60 mm in position 3 acquires maximum area. Finally, a small window size has little effect on flame front development. Therefore, the curves that correspond to window position 1 and position 3 are very close to each other.

The least explosion duration naturally occurs with the window diameter of 60 mm located in position 1. Combustion area in the second part of the process is fairly large as compared to other explosion scenarios. However, due to the fact that combustion products are discharged in this case, the chamber pressure is low.

It is evident that with the window diameter of 20 mm the curves of flame front area behavior are close to each other and approach the confined volume curve. With the window diameter of 60 mm, dynamics of flame front development is fundamentally different for different window positions.

Conclusion

Two critically important factors affect how a gas explosion develops in a chamber with a window. They are: window size and its position relative to the ignition location. Previously their combined effect on the process has been interpreted as follows: the larger the window size and the smaller the distance between the window and gas mixture ignition location, the lower the maximum explosion pressure. However, only the first part of the statement proves to be valid: the larger the window size, the lower the explosion pressure. As far as the effect of window location on explosion pressure is concerned, it is ambivalent. For larger window sizes, this well-known statement remains true, but reducing its size results in leveling out its location effect. Moreover, it turns out that with the window position located close to the ignition point, the pressure is even slightly higher than with a window positioned remotely. The explanation of this phenomenon lies in the specifics of flame front development, its area and visible movement velocity.

REFERENCES

- 1. Yu. Kh. Polandov, A. Ya. Korolchenko, S. A. Dobrikov. Gas explosion in a room with a window and passage to an adjacent room. *MATEC Web of Conferences*, 2016, vol. 86, article no. 04031, 7 p. DOI: 10.1051/matecconf/20168604031.
- 2. Yu. Kh. Polandov, S. A. Dobrikov, D. A. Kukin. Results of tests pressure-relief panels. *Pozharo-vzryvobezopasnost/Fire and Explosion Safety*, 2017, vol. 26, no. 8, pp. 5–14 (in Russian). DOI: 10.18322/PVB.2017.26.08.5-14.
- 3. C. R. Bauwens, J. Chaffee, S. B. Dorofeev. Effect of ignition location, vent size, and obstacles on vented explosion overpressures in propane–air mixtures. *Combustion Science and Technology*, 2010, vol. 182, issue 11-12, pp. 1915–1932. DOI: 10.1080/00102202.2010.497415.
- 4. C. R. L. Bauwens, J. M. Bergthorson, S. B. Dorofeev. Experimental investigation of spherical-flame acceleration in lean hydrogen-air mixtures. *International Journal of Hydrogen Energy*, 2017, vol. 42, issue 11, pp. 7691–7697. DOI: 10.1016/j.ijhydene.2016.05.028.
- 5. H. N. Phylaktou, G. E. Andrews, P. Herath. Fast flame speeds and rates of pressure rise in the initial period of gas explosions in large L/D cylindrical enclosures. *Journal of Loss Prevention in the Process Industries*, 1990, vol. 3, issue 4, pp. 355–364. DOI: 10.1016/0950-4230(90)80005-u.
- 6. Mingshu Bi, Chengjie Dong, Yihui Zhou. Numerical simulation of premixed methane–air deflagration in large L/D closed pipes. *Applied Thermal Engineering*, 2012, vol. 40, pp. 337–342. DOI: 10.1016/j.applthermaleng.2012.01.065.
- 7. J. Chao, C.R. Bauwens, S.B. Dorofeev. An analysis of peak overpressures in vented gaseous explosions. *Proceedings of the Combustion Institute*, 2011, vol. 33, issue 2, pp. 2367–2374. DOI: 10.1016/j.proci. 2010.06.144.
- 8. V. Molkov, V. Shentsov. Numerical and physical requirements to simulation of gas release and dispersion in an enclosure with one vent. *International Journal of Hydrogen Energy*, 2014, vol. 39, issue 25, pp. 13328–13345. DOI: 10.1016/j.ijhydene.2014.06.154.
- 9. B. M. Fakandu, G. E. Andrews, H. N. Phylaktou. Vent static burst pressure influences on explosion venting. In: *Proceedings. Tenth International Symposium on Hazard, Prevention and Mitigation of Industrial Explosions (XISHPMIE) (10–14 June 2014, Bergen, Norway)*. 16 p. Available at: http://eprints.whiterose.ac.uk/104968/1/X%20ISHPMIE%20Paper%20150%20GEA%205.pdf (Accessed 1 March 2019).
- 10. R. G. Zalosh. Gas explosion tests in room-size vented enclosures. In: *Proceedings of the 13th Loss Prevention Symposium*. Houston, 1979, pp. 98–108.
- 11. Yu. Kh. Polandov, M. A. Barg, S. A. Vlasenko. Simulation of combustion of gas-air mixture by the method of large particles. *Pozharovzryvobezopasnost/Fire and Explosion Safety*, 2007, vol. 16, no. 3, pp. 6–9 (in Russian).
- 12. A. A. Komarov, E. V. Bazhina. Determining the dynamic load caused by accidental explosions affecting buildings and structures of hazardous areas. *Vestnik MGSU / Proceedings of Moscow State University of Civil Engineering*, 2013, no. 12, pp. 14–19 (in Russian).
- 13. A. A. Komarov, G. V. Chilikina. Conditions of explosive mixture formation in residential houses with gas heating systems. *Pozharovzryvobezopasnost/Fire and Explosion Safety*, 2002, vol. 11, no. 4, pp. 24–28 (in Russian).
- 14. V. V. Mol'kov, V. P. Nekrasov. Dynamics of gas combustion in a constant volume in the presence of exhaust. *Combustion, Explosion, and Shock Waves*, 1982, vol. 17, issue 4, pp. 363–369. DOI: 10.1007/bf00761201.
- 15. E. Yu. Salymova. *Dynamics of development of dangerous factors in buildings with enclosing structures made of sandwich panels in fires and explosions*. Cand. Sci. (Eng.) Diss. Moscow, 2014. 110 p. (in Russian).
- 16. Jingde Li, Francisco Hernandez, Hong Hao, Qin Fang, Hengbo Xiang, Zhan Li, Xihong Zhang, Li Chen. Vented methane-air explosion overpressure calculation A simplified approach based on CFD. *Process Safety and Environmental Protection*, 2017, vol. 109, pp. 489–508. DOI: 10.1016/j.psep.2017.04.025.
- 17. Yu. Kh. Polandov, M. A. Barg, S. S. Markov. *Modeling of processes of burning and explosion of the gas mixes "Vulcan-M"*. Certificate of state registration of the computer program RU, no. 2007614950, publ. date 3 December 2007 (in Russian).
- 18. M. Barg. *Chislennoye i fizicheskoye modelirovaniye vzryvov gazovykh smesey* [Numerical and physical modeling of gas mixture explosions]. Saarbrucken, Germany, LAP Lambert Academic Publishing, 2011. 116 p. (in Russian).

- 19. O. M. Belotserkovskiy, Yu. M. Davydov. *Metod krupnykh chastits v gazovoy dinamike. Vychislitelnyy eksperiment* [The method of large particles in gas dynamics. Computational experiment]. Moscow, Nauka Publ., 1982. 392 p. (in Russian).
- 20. O. M. Belotserkovskii, Yu. M. Davydov. A non-stationary "Coarse particle" method for gas-dynamical computations. *USSR Computational Mathematics and Mathematical Physics*, 1971, vol. 11, no. 1, pp. 241–271. DOI: 10.1016/0041-5553(71)90112-1.
- 21. Yu. M. Davydov (ed.). *Chislennoye issledovaniye aktualnykh problem mashinostroyeniya i mekhaniki sploshnykh i sypuchikh sred metodom krupnykh chastits* [Numerical study of actual problems of mechanical engineering and mechanics of solid and granular media by the method of large particles]. Moscow, National Academy of Applied Sciences Publ., 1995. 1658 p. (in Russian).

Received 3 March 2019; received in revised form 8 April 2019; accepted 10 April 2019

Information about the authors

Iurii Kh. POLANDOV, Dr. Sci. (Eng.), Professor, Head of Scientific-Educational Center "Fluid Mechanics. Combustion", Orel State University named after I. S. Turgenev, Orel, Russian Federation; ORCID: 0000-0003-2983-6023, e-mail: polandov@yandex.ru

Sergey A. DOBRIKOV, Researcher, Orel State University named after I. S. Turgenev, Orel, Russian Federation; Software Designer, MERA, Nizhniy Novgorod, Russian Federation; ORCID: 0000-0002-9339-1500, e-mail: dobrikov@yandex.ru